ACS APPLIED MATERIALS & INTERFACES

Research Article

www.acsami.org

Sol–Gel Synthesis and Characterization of Silica Polyamine Composites: Applications to Metal Ion Capture

Jesse J. Allen,[†] Edward Rosenberg,*[,†] Erik Johnston,[†] and Carolyn Hart[‡]

[†]Department of Chemistry, University of Montana, Missoula, Montana 59801, United States

[‡]Purity Systems Inc., 1121 Broadway, Missoula, Montana 59812, United States

Supporting Information

ABSTRACT: A sol–gel method has been developed for the synthesis of composite materials analogous to the previously reported and commercialized silica polyamine composite (SPC) materials made from amorphous silica. Monolithic xerogels were formed using a two-step procedure with no templating agent using acid catalyzed followed by base catalyzed hydrolysis. This reaction was followed by ^{1}H NMR. Initial sol–gels were formed using a methyltrimethoxysilane (MTMOS) and 3-chloropropyltrimethoxysilane (CPTMOS) mixture. Elemental analyses and ^{13}C CPMAS NMR confirmed incorporation of both monomeric units into the surface structure. Some control over surface morphology was achieved by adjusting synthetic conditions. The resulting xerogels were reacted with poly(allylamine) (PAA) to give composite materials which showed much lower metal ion capacities than the commercially available amorphous silica analogs. The low degree of reaction of the chloropropyl groups indicated they were not surface-available to the polyamine. Addition of tetramethoxysilane (TMOS) produced a structural matrix and resulted in higher chloride utilization (reaction of surface chloropropyl groups with the polyamine). The ratio of the three siloxane monomeric components was varied until the resulting polyamine composite xerogels had metal capacities comparable with the commercialized SPC materials. These composites had narrower average pore size distributions and fewer small pores. Further modification of these composites with metal selective ligands showed material characteristics similar to those of commercially available SPC materials. Subjecting a composite made by the sol–gel route to one thousand load-strip cycles with Cu^{2+} shows essentially no loss in metal capacity, and this robustness compares favorably with that observed for the SPC made from amorphous silica gels.

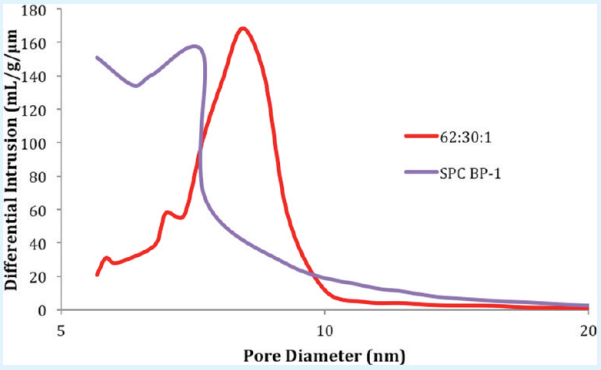

KEYWORDS: *sol–gel, composite materials, chemical synthesis, NMR, surface properties*

INTRODUCTION

Solid phase hybrid materials are finding an increasingly wide range of applications in device design, environmental monitoring, separations science, and catalysis.[1−11] Amorphous silica gels and sol–gels combined with polymers define a major portion of these hybrid materials for all these applications.[2−4,6−9] These silica based organic–inorganic materials offer a rigid matrix with high porosity and good thermal stability.[10,11] Our own studies have focused on silica polyamine composites (SPC) and have led to a wide range of metal-selective materials that in most cases provide the high loading associated with polymer based materials while providing a more rigid, porous, and hydrophilic surface that does not shrink or swell.[12−25] These patented materials are now in use in medium to large scale metal recovery projects and promise to offer more efficient on-stream processing of mining leaches and waste streams.[26] Copper recovery is among the most industrially important mineral industries. It is normally done by chemical reduction or increasingly by solvent extraction followed by electrowhinning. These processes produce waste streams that can contain upward of 1 g/L of copper in the presence of excess ferric ion and other divalent metals. The SPC technology has been shown to recover the copper from these waste streams to levels of <1 mg/L while rejecting the ferric ion and other divalent metals at low pH (∼1).[12,18,23,26]

The current manufacturing process does present problems in that it relies on the use of halo-silanes that produce hydrogen chloride to obtain good surface coverage and the use of hydrocarbon solvents in this step to efficiently outgas HCl, a by product, which requires a scrubber.[22−25] In addition, the SPC materials produced by this method have several deficiencies that could be improved upon. Pore size distributions are very wide and vary from batch to batch. This limits effective surface area (large pores) and hinders kinetic accessibility by ions (small pores). The maximum surface coverage achieved by the current manufacturing process is about 55%. The sol–gel

Received: December 12, 2011
Accepted: February 24, 2012
Published: February 24, 2012

approach to the synthesis of the SPC materials could address these deficiencies and could provide a more environmentally benign synthesis. We recently reported a preliminary study on the synthesis of SPC using the sol−gel approach.[27] These initial studies showed promise for the further development of such materials, and we report here the results of these further studies.

This work and prior art[27,28] have shown that the condensation of two-component silica sols can proceed without favoring the condensation of individual monomeric units and that the reaction rates of individual components (self-polymerization) are only weakly related to the concentration of cross-condensed species. The prevalence of cross-polymerization makes it possible to incorporate tethers during the formation of sol−gel composites. The sol−gel method also offers a more complete surface coverage with alkyl silanes, and the lack of exposed surfaces could result in greater alkaline stability of the material.[27]

Porous silicas, made by the sol−gel method, have classically been controlled by the use of templating agents, and while this can be effective, the method also requires the removal of the template, which is an undesirable step often requiring calcination.[29−32] The recent work of Dong and Brennan has shown that morphological control of porous silica can be achieved using a two-step processing method which does not require the use of templates but can allow the tailoring of pore structure to desired sizes and distributions.[33]

We report here an attempt to systematically improve the characteristics of the sol−gel SPC materials by modifying the proportions of the monomeric units while also changing the conditions under which the polymerization, precipitation, and gelation occur. The methods described here are an attempt to increase understanding of pore formation processes. Increased understanding of conditions affecting pore formation will then hopefully lead to control of pore formation. Subsequent reaction with the polyamine is performed under the same conditions as for the commercially available SPC.[22−25]

Direct comparison of sol−gels with currently available SPC materials is also reported here, with solid-state multinuclear NMR used to define structural characteristics. Mercury porosimetry was also used to determine the average pore size distributions of the sol−gels and SPC materials, and the performance of sol−gel synthesized materials was measured by metal ion capture and selectivity and compared to SPC.

EXPERIMENTAL SECTION

Materials and Methods. All chemicals were purchased from Sigma-Aldrich and used as received unless otherwise noted. Alkoxysilanes for the sol−gel preparations were purchased from Gelest Inc. as well as Sigma-Aldrich. The methods of polymer binding to the sol−gel ligand modified BP-1 composites were unchanged from those using SPC materials; sample preparations from the sol−gel BP-1 of the composites BP-2 and CuSelect are given below.[22−25] Raw silica gel (10 nm average pore diameter, 250−600 μm particle size, 450 m^2/g surface area) was obtained from Qing Dao Mei Gow, Qing Dao, China. Poly(allylamine) PAA-15B (15,000 MW) was obtained from Summit Chemicals Inc., NJ, USA, as a 15% by weight aqueous solution.

Atomic absorption (AA) analyses were done on an S series Thermo Electron corporation AA spectrometer. Metal ion solutions were run in a 2% nitric acid solution and were diluted to give approximately 0.1−0.2 absorbance units. AA analysis was used to determine the metal ion remaining bound on the surface of composites by measurement of the difference between the total metal ion in the initial solution and the total metal ion in the filtrate and rinses. Acidified solutions (5% HCl/5%HNO_3) were used to test for silica leaching. Silica concentrations were measured with a PerkinElmer inductively coupled plasma atomic emission spectrophotometer (ICP). Standards were run every 10−15 samples, and the initial leach solutions were examined to make sure they contained no silica. Mercury porosimetry measurements were performed on a 9500 Micromeritics Autopore Series Mercury Porosimeter operating at a maximum pressure of 36 000 psi, corresponding to a minimum intrusion diameter of 5 nm. Elemental analyses were done by Galbraith Analytical Laboratories, Lexington, KY.

Scanning electron microscopy (SEM) was performed using a Hitachi S-4700 field emission scanning electron microscope at 3000× and 20 000× magnifications. Sample preparation consisted of placing the sample on a conductive carbon tab on an aluminum stub. When necessary, samples were lightly sputter coated with a gold/palladium coating using a Pelco Model 3 Sputter Coater from Ted Pella Inc. Redding, CA.

Solid-state ^{13}C and ^{29}Si CPMAS NMR were measured on a 500 MHz Varian NMR spectrometer using a 4 mm rotor with parameters described in the Supporting Information as Supplemental Table 1. Solution-state ^{1}H NMR was done with a 500 MHz Varian NMR.

Stock solutions of Cu^{2+} were prepared using $Cu(SO_4)\cdot 10H_2O$. Stock solutions of Cu^{2+} mixed with Fe^{3+} were prepared using $Cu(SO_4)\cdot 10H_2O$ and $Fe_2(SO_4)_3\cdot xH_2O$. Solution pH was adjusted from the intrinsic pH, where necessary, using hydrochloric acid or sodium hydroxide. Stripping and recovery of copper was achieved with 2 M H_2SO_4. Metal standards for AA/ICP analyses were obtained from Fisher Scientific Co.

Synthesis of Xerogels by the Sol−Gel Method. Sol−gel syntheses used the two step process modeled after the work of Dong and Brennan.[33] To a 50 mL polyethylene beaker was added 6 mL of MeOH and 3.7 mL of pH = 2 HCl solution. To this mixture was added 20 mL of a premixed solution in the desired ratios of methyltrimethoxysilane (MTMOS), 3-chloropropyltrimethoxysilane (CPTMOS), and tetramethoxysilane (TMOS) or tetraethoxysilane (TEOS). These monomeric units were included in varying molar ratios for different studies (7.5:1 MTMOS:CPTMOS; 4.25:7.5:1 MTMOS:CPTMOS:TEOS; and 4.25:7.5:1, 4.25:30:1, 15.5:30:1, 31:30:1, and 62:30:1 MTMOS:CPTMOS:TMOS).

After 1 h of magnetic stirring, 3.7 mL of 7 M ammonium hydroxide was added to each sol−gel reaction. Upon gelation of the materials, stirring was stopped, and the mixture was allowed to age overnight at room temperature. This step was followed by aging at 40 °C for 24 h, followed by aging at 100 °C for 24 h. The materials were then crushed with a mortar and pestle and sieved to the desired particle size range, 250−600 μm for comparisons with commercial materials, and 150−250 μm for some of the other studies. Solid-state CPMAS ^{13}C NMR was 50 ppm (propyl C(3)), 25 ppm (propyl C(2)), 10 ppm(propyl C(1)), and −6 ppm (Si-Me).

Tracking the Acid Catalyzed Sol Step via ^{1}H NMR. To a 20 mL polyethylene vial was added 600 μL of MeOH and 370 μL of pH = 2 HCl solution. To this was added 2 mL of premixed MTMOS and CPTMOS in a molar ratio of 7.5:1. The solution was mixed by pipetting and then inserted into an NMR tube. ^{1}H NMR spectra were taken every 3 min to track the progression of the acid catalyzed polymerization step.

Conversion of the Sol−Gel Xerogels to the Polyamine Composite BP-1. For gels with particle sizes of 150−250 μm, the reaction of the resulting sol−gels with PAA was done by placing 2.0 g of sol−gel in a 250 mL, three-neck round-bottom flask; 16 mL of methanol was added, and the mixture degassed for 5 min. 64 mL of 15% by volume PAA was then added. The reaction mixture was then heated to 60−70 °C and stirred for 48 h. The solution was decanted from the solid while still warm and then washed 5 times with 80 mL of water, 1 time with 80 mL of 1 M NaOH, 3 times with 80 mL of water, 2 times with 80 mL of MeOH, and 1 time with 80 mL of acetone. All washes were stirred for 15 min. After washing, the composite was dried overnight at 70 °C. For gels with particle sizes of 250−600 μm, the reactions of the resulting sol−gels with PAA were done by placing 5.0 g of sol−gel in a 250 mL, three-neck round-bottom flask; adding 8 mL

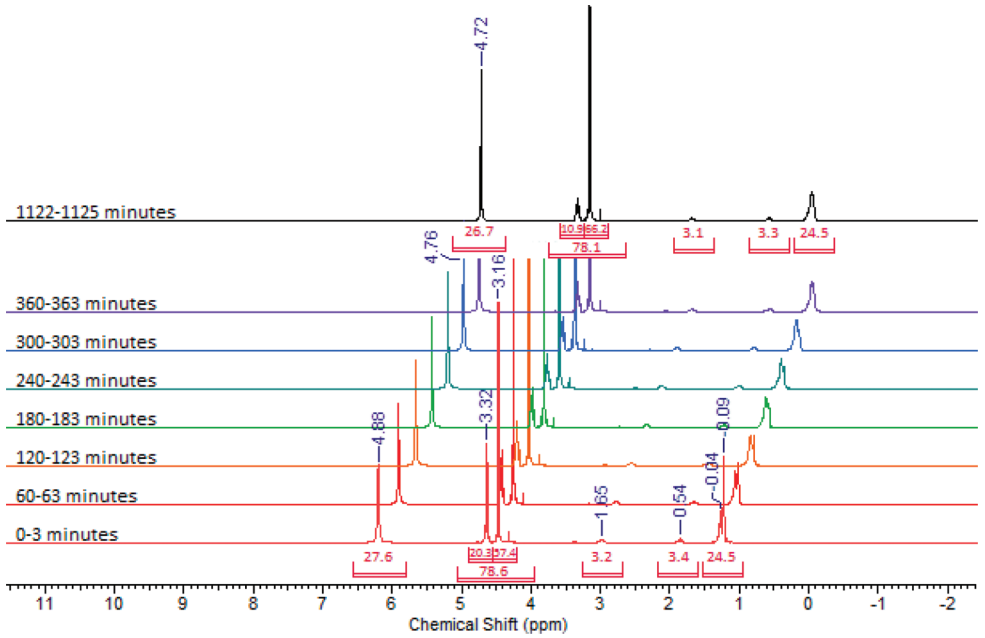

Figure 1. Solution-state ^{1}H NMR of a 7.5:1 molar ratio MTMOS:CPTMOS sol during the acid catalyzed stage at varying 3 min intervals. Peak intensities are normalized to the resonance furthest downfield.

of methanol; and degassing the mixture for 5 min. 32 mL of 15% by volume PAA was then added. The reaction mixture was then heated to 60−70 °C and stirred for 48 h. The solution was decanted from the solid while still warm and then washed 5 times with 40 mL water, 1 time with 40 mL 1 M NaOH, 3 times with 40 mL water, 2 times with 40 mL MeOH, and 1 time with 40 mL acetone. All washes were stirred for 15 min. After washing, the composite was dried overnight at 70 °C.

Copper capacities for the sol−gel composites were determined as described in the equilibrium batch experiment below. Elemental analyses for the sol−gels are included in Table 2. Solid-state CPMAS ^{13}C NMR was 50 ppm (propyl C(3)), 35 ppm (polymer CH and CH_2 25 ppm (propyl C(2))), 10 ppm (propyl C(1)), and −6 ppm (Si-Me).

Conversion of Sol−Gel Composites to the Metal Selective CuSelect and BP-2 Sol−Gel Composites.

CuSelect Preparation. The sol−gel composite BP-1 was placed in a three-neck, round-bottom flask and fitted with a condenser and an overhead stirrer. To this flask 4 mL per gram of composite of methanol was added and then allowed to sit for 5 min. The flask was then cooled in an ice bath for an additional 5 min. Then, 0.6 mL per gram of composite of pyridine-2-carboxaldehyde and 0.78 g per gram of composite of sodium triacetoxyborohydride was added to the flask while stirring. This was stirred for 1 h, while replenishing the ice bath when needed. After 1 h, another addition of 0.78 g per gram of composite of sodium triacetoxyborohydride was added to the flask while stirring was continued in the ice bath. The ice bath was allowed to come to room temperature, and the reaction was stirred overnight (18−20 h). The resulting CuSelect was then washed once with deionized water, three times with 5% by volume sulfuric acid, and then two times with methanol. The volume of the wash solutions was equal to the total volume of reaction solutions added to the flask, and the solutions were stirred for 15 min before the wash solution was removed through vacuum filtration using a stick frit. The modified sol−gel composite CuSelect was then dried overnight at 45 °C. A mass gain of ∼15% was seen with the conversion of BP-1 to CuSelect. Solid-state CPMAS ^{13}C NMR was 125, 145 ppm (aromatic), 50 ppm (ligand bound polymer CH and CH_2), 30 ppm (polymer CH and CH_2), and −6 ppm (Si-Me); propyl signals are obscured by the polymer.

BP-2 Preparation. The sol−gel composite BP-1 was placed in a three-neck round-bottom flask and was fitted with a condenser and overhead stirrer. To this flask, 2 g per gram of composite of sodium chloroacetate and 5 mL per gram of composite deionized water was added, and the mixture was stirred and degassed for 5 min. After the degassing, the reaction was stirred and heated to 65 °C overnight and the pH was monitored and maintained at basic levels using 8 M sodium hydroxide. The resulting BP-2 was then washed three times with deionized water, once with 2 M sulfuric acid, three times with deionized water, and two times with methanol. The wash volume was equal to the volume of reaction solution added to the flask, and all washes were stirred for 15 min before the wash solution was removed through vacuum filtration using a stick frit. The resulting modified sol−gel composite BP-2 was then dried overnight at 70 °C. A mass gain of ∼8% was seen with the conversion of BP-1 to BP-2. Solid-state CPMAS ^{13}C NMR was 168 ppm (carboxylate), 55 ppm (ligand bound polymer CH and CH_2), 30 ppm (polymer CH and CH_2), and −6 ppm (Si-Me); propyl signals are obscured by the polymer.

Method for Calculating the Number of Surface Anchor Points per Polymer Molecule. The calculation of the number of surface anchor points per polymer molecule was performed using chlorine and nitrogen elemental analyses of the CP gels and corresponding BP-1s. The method for the calculations has been previously published[16] but is also included in the Supporting Information (Supplemental Figure 1).

Equilibrium Batch Experiments. Batch extraction tests were conducted by adding 100 mg of SPC to 10 mL of metal solution at selected pH values. All batch extractions were done in triplicate. To ensure equilibration, the metal ion and SPC mixtures were placed in a shaker bath. After 24 h, the mixtures were allowed to settle. The supernatant was sampled and diluted using a 2% nitric acid solution for analysis using the AA method.

Breakthrough Column Experiments. Breakthrough column experiments on CuSelect were conducted by packing a 5 mL plastic syringe column fitted with frits on both ends and packed with 3.3 g of composite. The columns received flow from a variable flow FMI Lab Pump, Model QG150 from Fluid Metering Inc., NJ. The flow rate was 0.15 column volumes/minute. The column was tested for metal ion extraction by passing the following solutions in order: (1) 25 mL of pH = 1.5 DI H_2O (adjusted with HCl); (2) 300 mL of pH = 1.5 aqueous solution of 1.7 g/L Fe^{3+} and 0.5 g/L Cu^{2+}; (3) 20 mL of DI H_2O; (4) 70 mL of 2 M H_2SO_4; (5) 20 mL of DI H_2O.

The breakthrough column experiment on BP-2 was conducted by packing a 10 mL adjustable Omnifit glass column with 3.3 g of composite. The columns received flow from a variable flow FMI Lab Pump, Model QG150 from Fluid Metering Inc., NJ. The flow rate was 0.15 column volumes/minute. The column was tested for metal ion

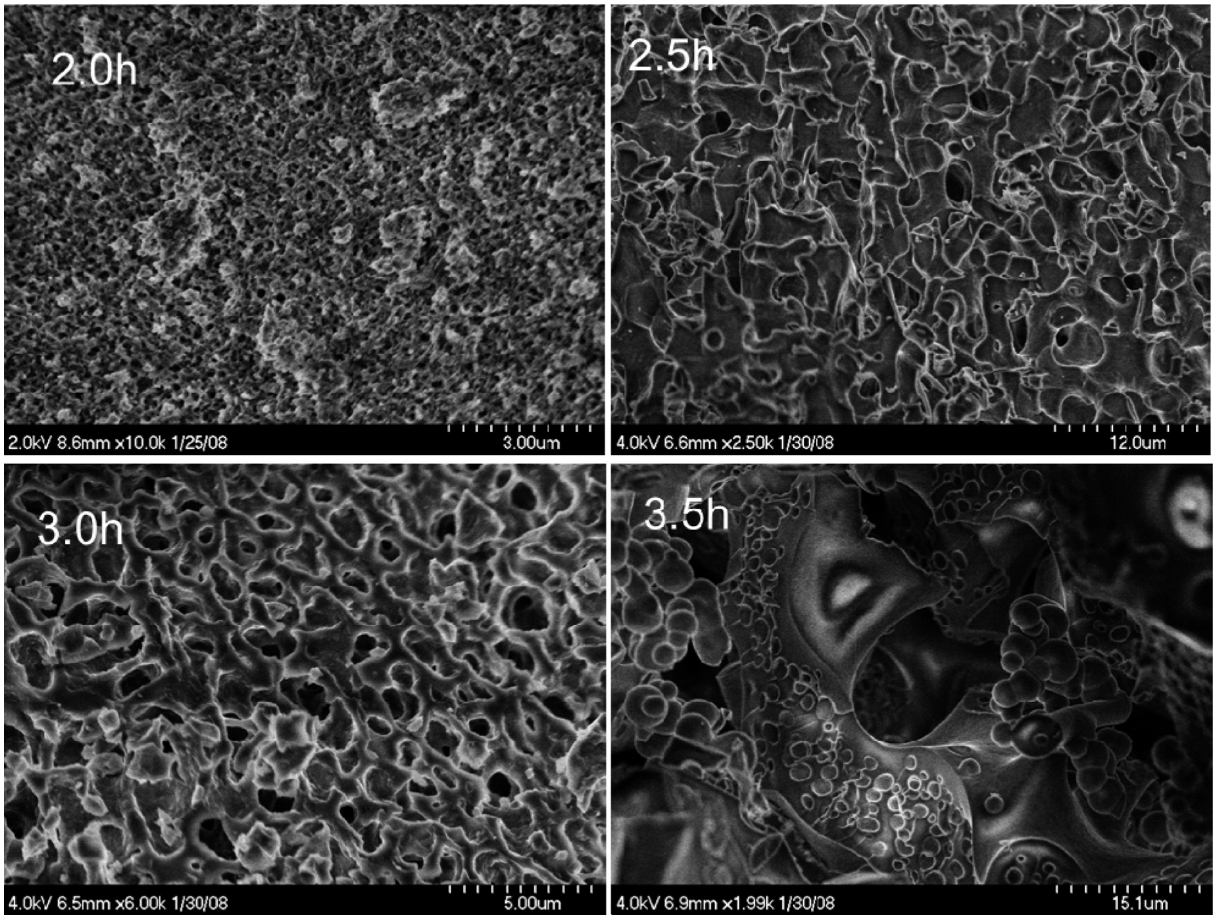

Figure 2. SEM images varying times in the acid catalyzed step showing the formation of a collapsed pore structure at very long acid exposures. Times of gelation were from 12 to 17 min.

extraction by passing the following solutions in order: (1) 25 mL of pH = 2 DI H_2O (adjusted with HCl); (2) 170 mL of pH = 2 aqueous solution of 1.5 g/L Ni^{2+} and 1.5 g/L Cu^{2+}; (3) 25 mL of DI H_2O; (4) 50 mL of H_2SO_4; (5) 25 mL of DI H_2O. Fractions were taken every 10 mL and measured for metal ion content by AA analysis.

Silica Leaching Protocol. Silica leaching samples were prepared as previously reported[27] using 9.5 mL of a pH = 10 NaOH solution and 0.5 mL of methanol. The mixtures were analyzed for concentration of silicon via ICPAES. All leaching experiments were done in triplicate, and the error bars are based on the standard deviations of the triplicate data.

Longevity Testing Protocol. BP-2 longevity was studied using the following procedure with 3.18 g of 62:30:1 TMOS:MTMOS:CPTMOS sol–gel BP-2 with a bed volume (BV) of 5.5 mL in a 10 mm diameter, 12 cm glass Omnifit column: (1) pre-conditioning, hydrate resin with 5.5 mL of DI H_2O, wash with 5.5 mL of 20% sulfuric acid, and rinse with 27.4 mL of DI H_2O; (2) breakthrough Cu capacity test (after 0, 1, 107, 522, and 1000 cycle tests; flow rate: 0.15 BV/min), (a) condition with 5.5 mL of DI H_2O and then 5.5 mL of 25% sulfuric acid, rinse with 27.4 mL of DI H_2O, (b) load, Cu feed (3000 mg/L, pH 2.0, 90 mL), (c) load wash, DI H_2O, 15 mL, (d) elute, 25% sulfuric acid, 15 mL, (e) elute rinse, DI H_2O, 15 mL; (3) cycle test, Cu breakthrough (repeated 1000 cycles; flow rate: 2.4 BV/min), (a) load, Cu feed (3000 mg/L, pH 2.0, 9.3 mL), (b) elute, 25% sulfuric acid, 13.7 mL (2.5BV), (c) rinse, DI H_2O, 13.7 mL (2.5BV). Details of copper analyses and the order of cycles can be found in Supplemental Table 2, Supporting Information.

RESULTS AND DISCUSSION

Tracking Polymerization via NMR. The sol–gels reported here have been synthesized by the two-step method previously outlined by Dong and Brennan, using an initial acid catalyzed step and a following base catalyzed step.[33] Initial studies of the sol–gel polymerization focused solely upon the use of the monomers (MTMOS and CPTMOS) to investigate the effects that each stage of the polymerization has upon reaction progress. The initial studies utilized a molar ratio of 7.5:1 for MTMOS:CPTMOS which was chosen based upon previous work.[14−16]

The initial, acid catalyzed step of the reaction involves rapid hydrolysis of the monomers to form low molecular weight oligomers and linear chain oligomers. This reaction has been previously monitored by solution phase ^{29}Si NMR.[28] However, ^{1}H NMR can also be used to follow reaction progress, as seen in Figure 1. When a system where two alkyltrialkoxysilanes are present is used, the ^{29}Si NMR spectral lines for the individual species are indistinguishable by solid-state CPMAS NMR. In solution ^{1}H NMR, the changes in the intensities of the methoxy CH_3 relative to the methanol CH_3 can be used to monitor reaction progress. This represents a more convenient way to follow a mixed alkyltrialkoxysilane polymerization.[28,34]

Figure 1 illustrates the progress of the polymerization with time. The furthest upfield resonance(s) (0.0–0.2 ppm) represent H–C–Si bound protons. It can be seen that, as the reaction proceeds, the peaks here merge as a result of the formation of Si–O–Si bonds creating multiple environments. The resonances at 0.7 and 1.8 ppm represent the CH_2 and CH_2Cl of the chloropropyl group. The unique chloropropyl peaks are seen to maintain constant intensity and chemical shift

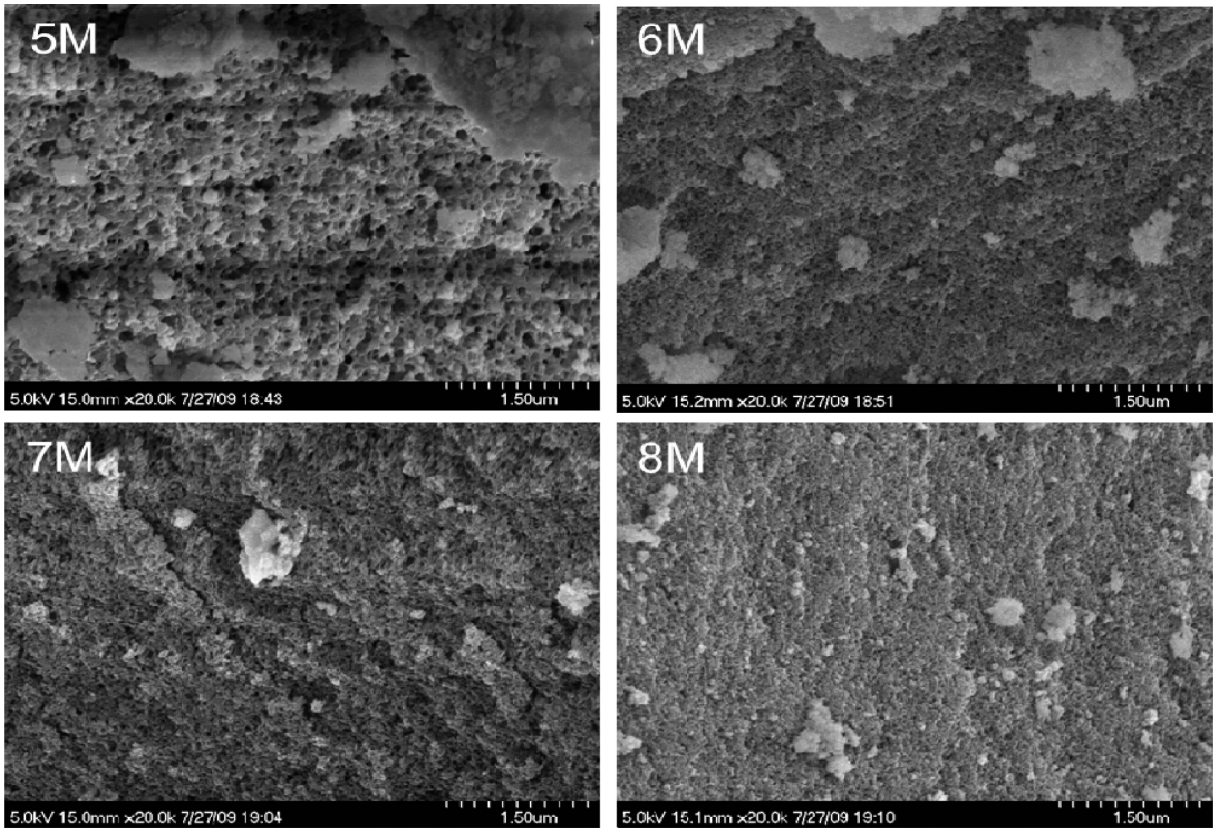

Figure 3. SEM images showing the formation of smaller pores with increased base concentration. Times of gelation were from 30 s to 17 min.

throughout the reaction, as would be expected from their distance to the reactive centers. At 3.3 and 3.45 ppm, resonances are seen representing the CH_3 on MeOH and Si−O−Me groups, respectively. The sum of the integrations of these peaks remains constant over time, with the MeOH peak increasing in intensity while the Si−O−Me peak decreases in intensity proportionally. The furthest downfield resonance is assigned as a hydroxyl group from the combination of methanol and water. It can be seen that, as the reaction progresses, the OH resonance shifts from 5.0 to 4.95 to 4.85 ppm at times of 7, 49, and 1122 min, respectively. This increased shielding is a result of the increased concentration of methanol released from the hydrolysis of Si−O−Me bonds.

The Effect of the Acid Catalyzed Step on Pore Formation. As the polymerization progresses in the acid catalyzed step, oligomeric chains grow longer. Upon transition to the base catalyzed step, aggregation of the oligomers is promoted. This aggregation is faster than during the acid catalyzed step, with the larger clusters reacting more rapidly, leading to broader average pore size distributions. The larger clusters agglomerate throughout the entire solution, leading to decreased flow and eventually gelation. This effect, in conjunction with solvent hydrogen bonding effects, then leads to pore formation and definition.[33] Using shorter times for the acid catalyzed step results in smaller pores due to the aggregation of smaller clusters, though at very short times in acid (t_a < 1 h), a flocculated, nonporous precipitate forms without gelation. Larger pores form as the time in acid increases. However, at very long times in acid (t_a > 3 h), a nonporous resin forms due to high levels of chain cyclization, as seen in Figure 2. At 3.0 h, the material formed with gelation; however, the pores formed were rather large, on the micrometer scale, and had high variability in diameter.

The Effect of the Base Catalyzed Step on Pore Formation. The base catalyzed step utilized in the synthesis of sol−gels is a faster process promoting the reaction of more highly substituted Si centers as well as cluster−cluster binding, leading to increased cluster sizes and eventually a single cluster spanning the entire solution, restricting flow to the point where gelation occurs.[34] The properties of the resulting gel show a dependence upon the length of time between base addition and gelation, which can be partially controlled by the concentration of base during this step in the catalysis. At low concentrations of base, gel formation proceeds at a slower rate, resulting in increased pore size, as seen in Figure 3. At a 5 M base concentration, it is observed that pore size diameters are relatively large, larger than desired for further modifications with polyamines. At 6 M base concentration, pore sizes are decreased, and at 7 and 8 M base concentrations, pore size diameters appeared approximately equivalent and in the range desired for materials with characteristics designed for ion exchange.

The Effect of Tetraalkoxysilane Addition on Material Characteristics. The materials made using only alkyltrialkoxysilyl monomeric units showed that it was possible to exercise some control over the characteristics of pores formed during the polymerization process. Upon PAA addition to form BP-1, however, the best of these materials showed only 87.1 mg/g copper batch capacities. Repeated syntheses showed poor reproducibility, resulting in average pore diameters ranging from 9 to 13.6 nm and copper capacities ranging from 41.5 to 87.1 mg/g.[27] A proposed reason for the difficulty in

reproducing the materials is internalization of the hydrophobic alkyl groups present in the alkyltrialkoxysilanes.[32,36]

The SPC materials tested have so far shown very long usable lifetimes, with <10% capacity loss in more than 3000 copper loading–acid stripping–base regeneration cycles.[37] Much of this stability is attributed to the multiple point covalent anchoring of the polyamine to the surface and to the bulk silica matrix which provides increased mechanical stability. It was thought that the addition of a tetraalkoxysilane to the reaction mixture would not only increase mechanical stability through cross-linking but also may increase the reproducibility of the sol–gel reaction and expose more of the chloropropyl silanes to reaction with PAA.[30,31,38–41]

Initial introduction of tetraalkoxysilanes was attempted using TMOS and TEOS; however, TEOS did not fully react under the experimental conditions tried, and it was found that TMOS was a more suitable monomer for the intended purpose.[27] Initial reactions used a 4.25:7.5:1 TMOS:MTMOS:CPTMOS ratio in an attempt to form a structure that utilized all the alkoxide groups.

^{13}C NMR of the resulting composite made from this material suggests the same rates of incorporation of all of the monomeric units, despite their different rates of self-polymerization. This is evidenced by the splitting of the halocarbon resonance on C_3 of the chloropropyl group as seen in Figure 4.

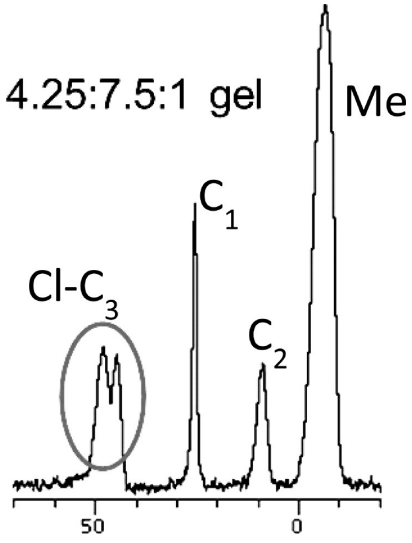

Figure 4. ^{13}C CPMAS NMR of sol–gel with a TMOS:MTMOS:CPTMOS molar ratio of 4.25:7.5:1, with the halocarbon resonance circled to emphasize splitting.

This splitting is assigned to a neighboring group effect and is present in commercial SPC materials with mixed silanes but not in those utilizing only 3-chloropropyltrichlorosilane as the monomer for surface silanization. This then suggests that two main environments for the 3-chloropropyl groups are (1) having one or more neighboring 3-chloropropyl groups and (2) having only neighboring methyl surface groups. Predominant agglomeration of 3-chloropropyl groups would result in this resonance not being split.[36]

Copper capacities of materials using the 4.25:7.5:1 ratio still varied significantly, ranging from 68.7 up to 100 mg/g. It was found that the reaction of PAA with the chloropropyl group was incomplete, with only 35–38% of surface halocarbons being reacted. Though this resulted in multipoint anchoring at ~38 anchors per polymer molecule on average, the low level of chloride utilization (reaction of surface chloropropyl groups with the polyamine) further supports the concept that nonpolar alkyl groups were being internalized into the support matrix. Gels made with increasing amounts of MTMOS resulted in decreased chloride utilization, down to 31% on a gel made with 4.25:30:1 TMOS:MTMOS:CPTMOS. Copper batch capacities decreased with increasing ratios of MTMOS to CPTMOS.

The Effect of Increasing TMOS to Make Halocarbons Surface Available. The low chloride utilization observed prompted us to investigate further increasing the relative concentration of TMOS, increasing internal framework density and "pushing" the nonpolar alkyl groups to the surface, effectively increasing the number of halocarbons available for nucleophilic attack by PAA. This increased cross-linking and internal framework development can be followed by the solid-state ^{29}Si NMR spectra of sol–gels with increasing relative amounts of TMOS in Figure 5.

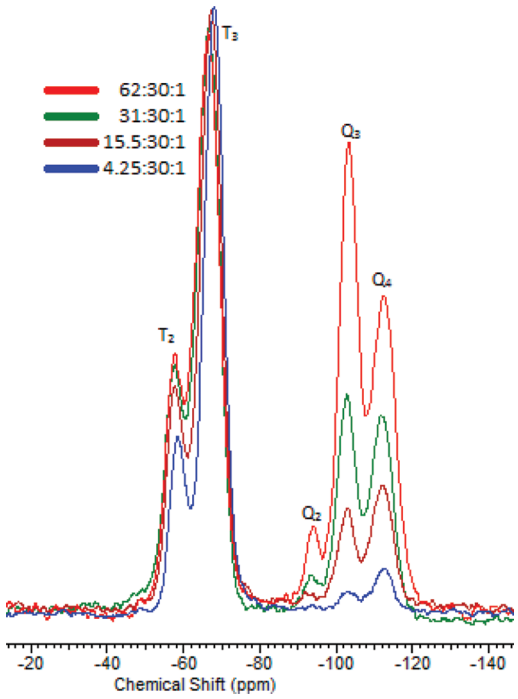

Figure 5. ^{29}Si NMR showing increasing internal framework with increasing relative amounts of TMOS, with ratios given as TMOS:MTMOS:CPTMOS. Peak intensities are normalized to the T_3 resonance.

The nomenclature used for the identifiable ^{29}Si NMR resonances are shown in Chart 1.[13,27] Q_4 species represent Si atoms with four Si–O–Si bonds. Q_3 species represent atoms of Si with three Si–O–Si bonds and one Si–O-R bond where R can be a hydrogen or alkyl group. Q_2 species represent atoms of Si with two Si–O–Si bonds and two Si–O-R bonds. Q_1 species represent atoms of Si with one Si–O–Si bond and three Si–O-R bonds. T_3 species represent atoms of Si with three Si–O–Si bonds and one Si-R′ bond where R′ is an alkyl group. T_2 species represent atoms of Si with two Si–O–Si bonds, one Si-R′ bond, and one Si–O-R bond. T_1 species represent atoms of Si with one Si–O–Si bond, one Si-R′ bond, and two Si–O-R bonds.[34,38,40]

The ^{29}Si NMR spectra in Figure 5 show that increasing TMOS results in increasing intensities of Q peaks (those

dx.doi.org/10.1021/am201761m | ACS Appl. Mater. Interfaces 2012, 4, 1573–1584

Chart 1. Structures of Different Types of Silicon Sites in Composites, Where R Represents H or an Alkyl Group

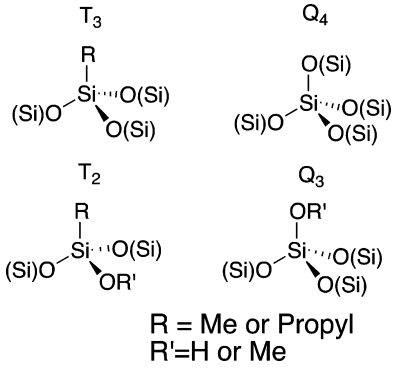

assigned to the bulk siloxane). In addition to this effect, there is also some broadening of the T resonances (those assigned to the alkyltrialkoxysilanes) and an increased T_2 peak intensity, suggesting less complete reaction of alkyltrialkoxysilanes. This effect does not persist upon polymer addition, however, as the matrix undergoes further reaction under the conditions of the reaction (heat and alkalinity), as evidenced by the disappearance of the T_2 resonance (vida infra).[25] Further evidence of this is shown in ^{29}Si NMRs of the BP-1s (Supplemental Figure 2, Supporting Information) made from the same composites shown in Figure 5.

Sol–gels were prepared using four mixtures with increasing molar ratios of TMOS relative to the other monomers. The four ratios chosen were 4.25:30:1, 15.5:30:1, 31:30:1, and 62:30:1 for TMOS:MTMOS:CPTMOS. BP-1 composites made from these gels showed several significant trends with improved characteristics as the level of TMOS increased. Both chloride utilization and copper binding of the resulting composites showed strong correlations with increasing amounts of TMOS (Figure 6). Chloride utilization in the commercially available SPC BP-1 was found to be ~80%. Chloride utilization for the sol–gel BP-1 materials made with increasing amounts of TMOS varied from 31 to 51%, still utilizing less of the surface anchors than materials made from amorphous silica (Table 1). Interestingly, however, this did not have a significant impact on polymer tethering, which was found to range from 12.2 to 13.3

Table 1. Copper Capacities, Chloride Utilizations, and Anchor Points for Sol–Gel BP-1 Materials with Varying Relative Amounts of TMOS

ratio of silanes (TMOS:MTMOS:CPTMOS)	anchor points per polymer molecule[a]	percent chloride utilization	batch copper capacity[b] (mg Cu/g composite)
4.25:7.5:1	37.7	38	100
4.25:30:1	13.3	31	52
15.5:30:1	12.8	36	83
31.0:30:1	12.2	41	84
62.0:30:1	12.5	51	118

[a]Number of anchor points per molecule of polymer and percent chloride utilization calculated from the difference in Cl content before and after polymer grafting, %N and MW of polymer. [b]Batch capacity at pH = 3.5–4 for BP-1 in mg/g as measured by AA.

anchors per polymer molecule (Table 1). For the material with the highest molar ratio of TMOS, copper batch capacity was found to be 118 mg/g, which is slightly higher than the copper capacities found in amorphous silica SPC materials (95–105 mg/g) (Table 1). This observation is consistent with the internalization model proposed earlier, where increasing internal cross-linking increased the number of available halocarbons.[28,35]

Table 2 shows that elemental analyses on the different composites show higher levels of carbon, hydrogen, and chlorine relative to SPC materials, due to having less bulk silica framework. At very high ratios such as 62:30:1, this effect is diminished. All of the BP-1 materials showed increased amounts of carbon relative to the initial gels, and nitrogen is not observed prior to the addition of PAA to the composite surface.

Gelation and pore structure are also highly affected by the addition of TMOS. Figure 7 shows the effects of three different ratios of TMOS:MTMOS:CPTMOS upon the average pore size distribution. At very low amounts of TMOS, little porosity is observed and the average pore size distribution is relatively broad. The composite resulting from a 4.25:30:1 ratio of TMOS:MTMOS:CPTMOS showed this low level of porosity. As the amount of TMOS increases, porosity increases and pore sizes decrease. The composite resulting from a 31:30:1 ratio of

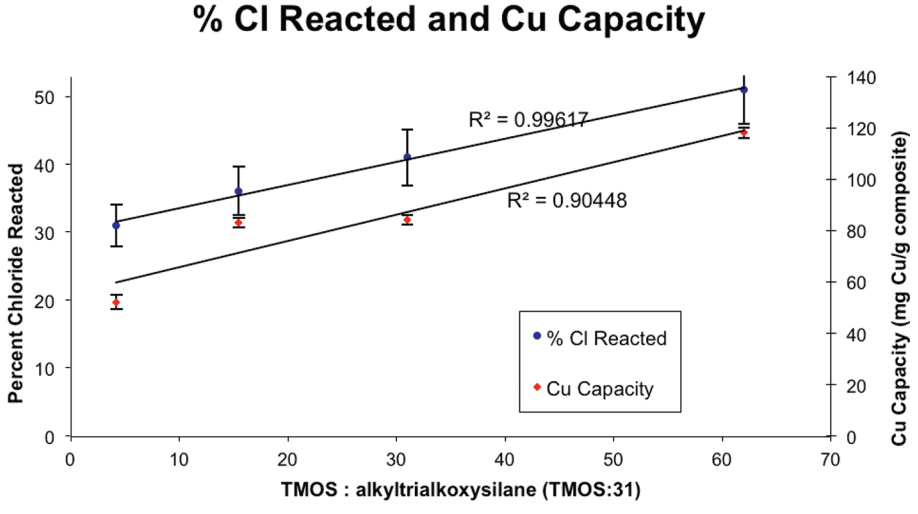

Figure 6. Copper capacities and chloride utilizations for sol–gel BP-1s with varying relative amounts of TMOS.

Table 2. Elemental Analyses, Copper Capacities, Chloride Utilizations, and Anchor Points for Conventional Silica Based Materials as well as Sol−Gels with Varying Monomeric Unit Composition

name of sample	%C	%H	%Cl	%N	anchor points/polymer molecule[a]	% chloride utilization[a]	copper capacity[b] (mg/g)
7.5:1 silanized gel	3.8	0.97	1.05	N/A	N/A	N/A	N/A
7.5:1 SPC BP-1	11.6	2.36	0.17	3.26	24	81	95−105
7.5:1 sol−gel	20.1	4.75	5.46	N/A	N/A	N/A	N/A
7.5:1 sol−gel BP-1	24.9	5.31	4.44	2.47	20	10	92
4.25:7.5:1 sol−gel	10.4	3.44	2.66	N/A	N/A	N/A	N/A
4.25:7.5:1 sol−gel BP-1	20.2	4.46	1.73	3.02	21	26	96
4.25:30:1 sol−gel	14.1	4.32	1.19	N/A	N/A	N/A	N/A
4.25:30:1 sol−gel BP-1	22.7	5.06	0.73	2.61	13	31	80
62:30:1 sol−gel	6.69	2.37	0.51	N/A	N/A	N/A	N/A
62:30:1 sol−gel BP-1	12.0	2.73	0.23	1.99	12.5	51	118

[a]Number of anchor points per molecule of polymer and percent chloride utilization calculated from the difference in Cl content before and after polymer grafting, %N and MW of polymer. [b]Batch copper capacity at pH = 3.5−4 for BP-1 in mg/g as measured by AA.

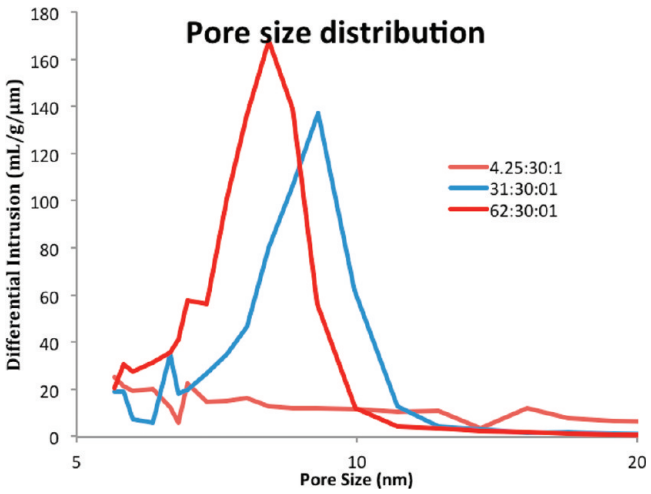

Figure 7. Average pore size distributions for sol−gels with varying relative amounts of TMOS.

TMOS:MTMOS:CPTMOS showed greatly increased porosity and much narrower average pore size distribution, with an average pore diameter of 9.1 nm. The composite resulting from a 62:30:1 ratio of TMOS:MTMOS:CPTMOS showed even higher porosity but a decreased average pore diameter of 8.0 nm. This is expected for materials having increased cross-linking. Additionally, the gelation times were seen to decrease with increasing levels of TMOS, which would result in smaller clusters agglomerating and the formation of smaller pores.

BP-2 and CuSelect Composite Characterizations and Performance. Further modification of polyamine composites provides the ability to design composites with ligands selective for certain metal separations. The picolylamine functionalized material, CuSelect, has been shown to be selective for copper over ferric ion and other divalent transition metals at low pH.[24,25] The aminoacetate functionalized materials (BP-2) have been shown to be effective for the separation of Cu^{2+} from Ni^{2+} at low pH.[16] In both, CuSelect and BP-2 the ligands are bidentate . The copper is likely square planar in both cases with water or sulfate filling out the coordination sphere in CuSelect. Two aminoacetates provide a square planar coordination sphere in the case of BP-2.[16] Some of the sites on BP-2 have two acetates on one amine, and these sites act as tridentate ligands.[16] Scheme 1 illustrates the synthesis of these two materials from BP-1. CuSelect is synthesized by the reaction of pyridine-2-carboxaldehyde and sodium triacetoxyborohydride in MeOH with the primary amines of BP-1. BP-2 is synthesized by reaction of sodium chloroacetate with BP-1 under basic conditions.

Ligand loading on the composites CuSelect and BP-2 is evidenced from the solid-state CPMAS ^{13}C NMR. All three materials (BP-1, CuSelect, and BP-2) show the resonance for the Si-Me group at −6.0 ppm. The three resonances corresponding to the 3-chloropropyl group can also be seen at 9, 23, and 44 ppm on the BP-1. The CuSelect and BP-2 show the Si−C_1 resonance from the 3-chloropropyl group at 9 ppm, but the other two resonances are overshadowed by the polyamine resonances. The polyamine can be seen as a broad resonance ranging from ∼25 to 45 ppm for the BP-1 and ∼20 to 40 ppm for the CuSelect and BP-2. The CuSelect shows a ligand bound polymer resonance at 48 ppm which is very broad, beginning at ∼40 ppm and then tailing off to ∼80 ppm. The ligand bound polymer resonance in BP-2 is seen ranging from ∼40 to 65 ppm with the apex at 56 ppm and a shoulder at ∼48 ppm. The aromatic carbons on CuSelect show two resonances: one ranging from ∼120 to 133 ppm and the other ranging from ∼133 to 160 ppm. The carboxylate group on BP-2 can be seen as a broad resonance from ∼160 to 175 ppm.

The SPC BP-2 made from amorphous silica has many doubly modified amine groups after reaction of BP-1 with chloroacetic acid. This BP-2 has ∼2.7 mmol ligand/g composite, while CuSelect has ∼2.0 mmol ligand/g composite.[16] This is significantly higher than the 0.4−1.1 and 0.7−1.0 mmol/g found for sol−gel materials made into BP-2 and CuSelect, respectively. Figure 8 shows the comparison of ligand loading and copper batch capacities for the ligand modified BP-1 composites CuSelect and BP-2. When comparing Figures 6 and 8, it can be seen that, with increasing relative amounts of TMOS, the BP-1 chloride utilization and copper batch capacity increase. This trend also carries through to ligand loading on modified composite materials.

CuSelect made from 4.25:7.5:1 TMOS:MTMOS:CPTMOS showed a ligand loading of 0.7 mmol ligand/g composite. This increased to 0.83 and 0.96 mmol ligand/g composite for 31:30:1 and 62:30:1 TMOS:MTMOS:CPTMOS ratios, respectively. BP-2 made from 4.25:7.5:1 TMOS:MTMOS:CPTMOS showed a ligand loading of 0.42 mmol ligand/g composite. This increased to 0.72 and 1.07 mmol ligand/g composite for 31:30:1 and 62:30:1 TMOS:MTMOS:CPTMOS ratios, respectively.

However, when a comparison of copper capacities at pH = 2 for BP-2 is made, the sol−gel materials show improved

Scheme 1. Synthesis of Ligand Modified Sol–Gel Composites[a]

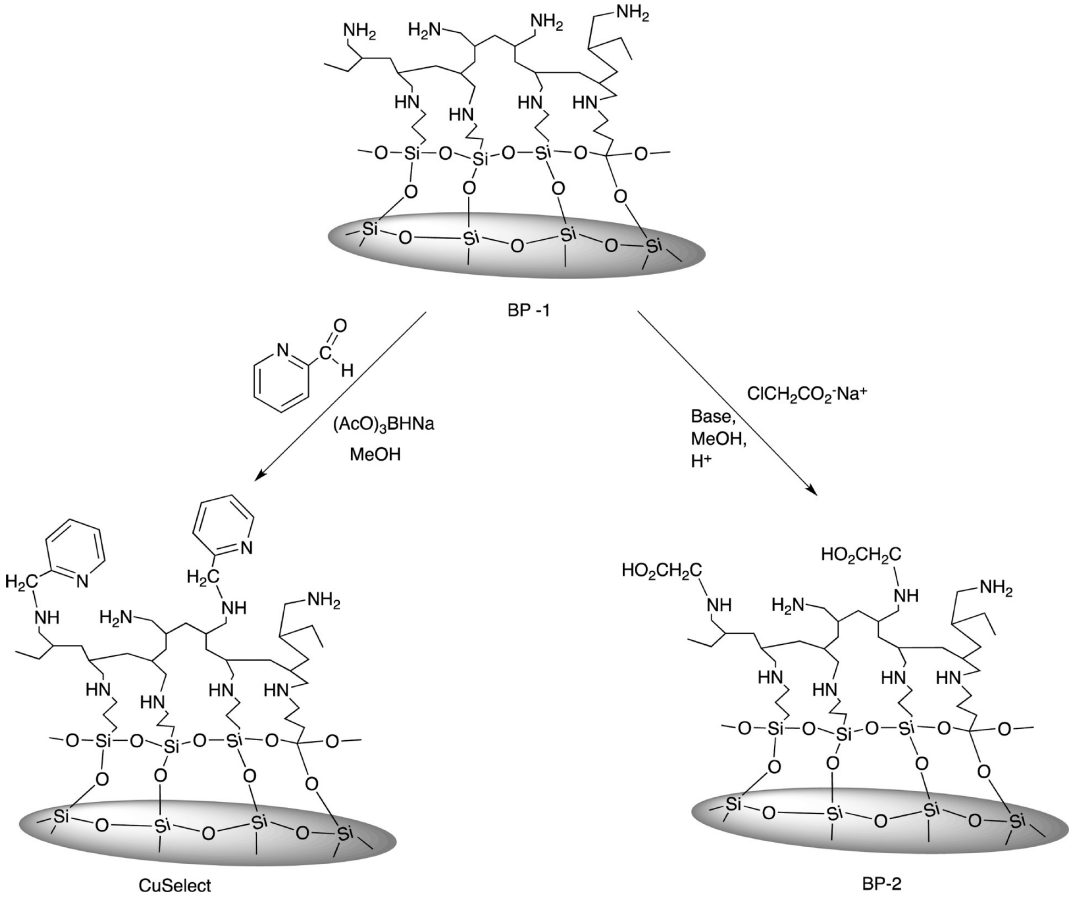

[a]Note: based on metal loading and analysis, not all amine sites are modified.

capacities over conventional materials (51 vs 38 mg/g). This is thought to be an effect of a decrease in the number of small pores, resulting in more availability for active sites after ligand modification. For CuSelect, however, the capacities at pH = 1.5 are somewhat lower (25 vs 35 mg/g), which is thought to be due to decreased ligand loading resulting from the bulky ligand being too large for the available average pore diameters seen in Figure 9.

The breakthrough experiments show metal capacities that are significantly decreased for both materials relative to SPC materials. BP-2 synthesized from sol–gels had Cu^{2+} capacities of 36 mg/g under breakthrough conditions in competition with Ni^{2+}. CuSelect synthesized from sol–gels had Cu^{2+} capacities of 15 mg/g under breakthrough conditions in competition with Fe^{3+}. BP-2 synthesized from sol–gels and SPC materials gave selectivities for Cu^{2+} over Ni^{2+} of 11:1 and 27:1, respectively. CuSelect from sol–gels and SPC materials gave selectivities for Cu^{2+} over Fe^{3+} of 40:1 and 67:1, respectively. The decreased selectivity for the ligand-modified sol–gel SPC materials is tentatively assigned to the decreased ligand loading, though further investigation is warranted.

The Effect of Polymer Binding on Gel Reorganization. Binding of PAA on the surface of the sol–gel composites is performed using a very similar procedure to that used for amorphous silica SPC composites. The conditions under which the polymer addition proceeds appear to result in further conversion of the T_2 sites to T_3 sites (Chart 1). This is evident by the decrease in Q_3 and T_2 peak intensities at −102 and −56 ppm, respectively, in the ^{29}Si NMR before and after polymer addition. It is proposed that this reorganization is due to the heating under aqueous, alkaline conditions.[27]

The Q_3 and T_2 resonances represent unreacted silanol or alkoxysilane sites. These sites are more receptive to alkaline attack, and their decreased level upon polymer addition is also corroborated by silica leaching studies.

The decreased leaching shown upon polymer grafting defines a fundamental difference between SPC and sol–gel materials. The surface of amorphous silica composites becomes more susceptible to alkaline attack upon modification with PAA.[27] This suggests that the materials made by sol–gel methods, though they show greater leaching than the conventional SPC materials prior to binding of PAA, have weaker surface interactions with PAA because of the better surface coverage by alkyl groups.[27]

SEM and Mercury Porosimetry of "Best" BP-1s. Polymer binding has been shown to lower both pore size and surface area. It is suggested that some of the decrease in surface area is due to the clogging of smaller pores[41] and that the formation of slightly larger pores relative to conventional silica could result in increased composite performance following polymer addition. The ability to design pores of specific sizes is a great advantage for an ion exchange material. As seen in Figure 7, conditions of the sol–gel reaction can be altered to achieve a level of control over pore formation. Figure 9 illustrates the differences between the most desirable sol–gel BP-1 to date (made from 62:30:1 TMOS:MTMOS:CPTMOS)

dx.doi.org/10.1021/am201761m | ACS Appl. Mater. Interfaces 2012, 4, 1573–1584

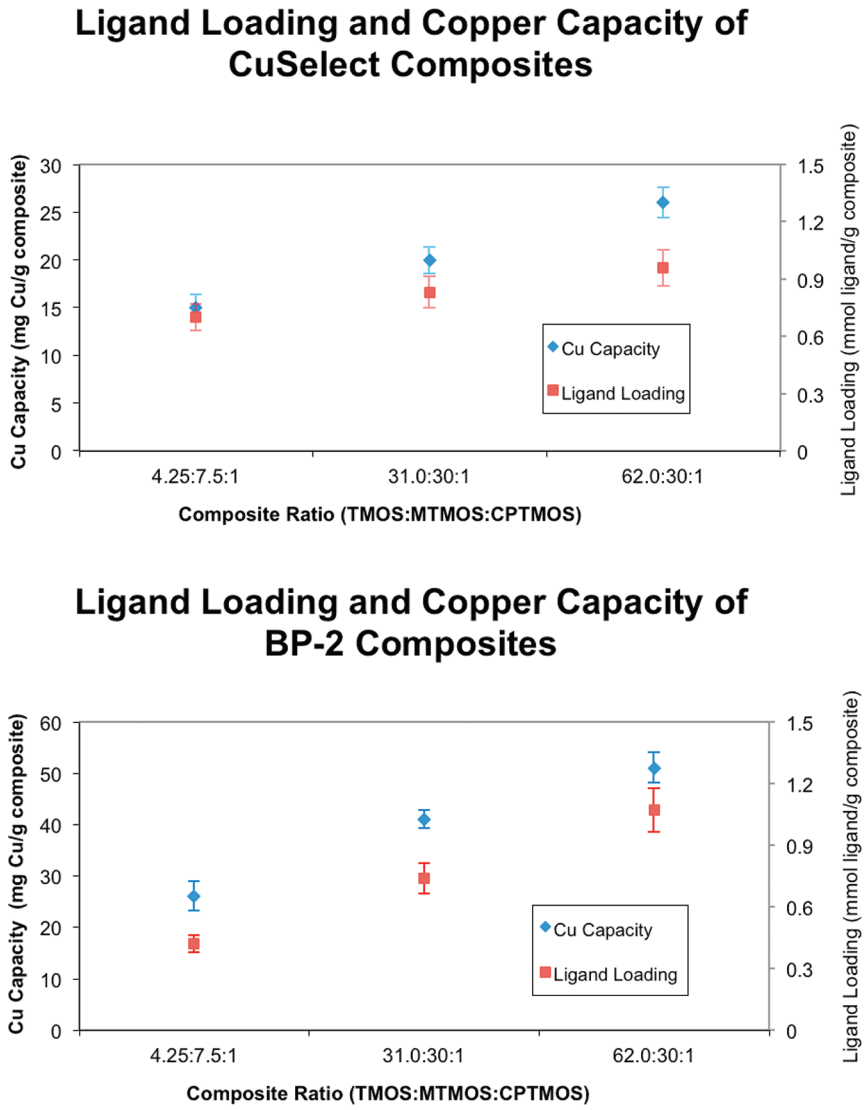

Figure 8. Ligand loading and copper batch capacity for sol–gel CuSelect and BP-2.

and a typical SPC BP-1. The sol–gel BP-1 demonstrates pore sizes with a narrower distribution than the conventional SPC materials. Conventional materials have many of their pores present in sizes smaller than the 5 nm minimum that can be measured by the mercury porosimeter used for these measurements. Many of these pores would become inaccessible upon polymer binding. The maximum average pore diameter of the amorphous silica BP-1 was 6.3 nm. The average pore diameter of 8.0 nm for the sol–gel BP-1 is closer to the desired range.

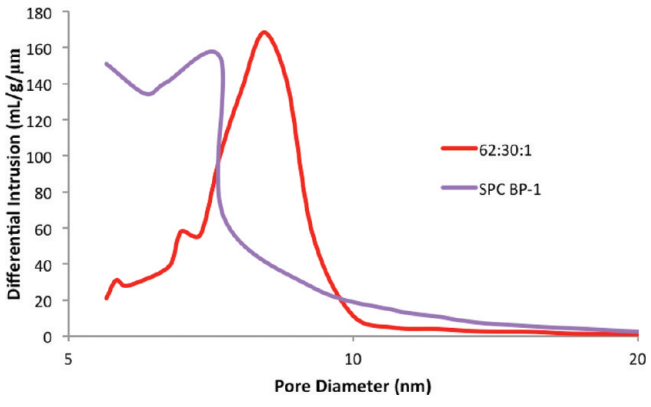

Figure 9. Average pore size distributions for SPC BP-1 and 62:30:1 TMOS:MTMOS:CPTMOS BP-1.

BP-1 Silica Leaching Comparison of SPC with 62:30:1 and Previous Materials. The susceptibility to silicate leaching under alkaline conditions is considered to be the greatest weakness of SPC materials. It was thought that, with sol–gel materials, some of this susceptibility could be avoided through both a decreased amount of bulk silica and the avoidance of "bare" silica surfaces which have not been silanized. Though both of these effects are observed in sol–gel composites, leaching increases upon dilution of chloropropyl anchors with methyl groups. The large increase in leaching from 9.2 to 36.0 ppm for the conventional SPC materials upon polymer addition is thought to be a direct result of polymer–surface interactions. The initial sol–gel experiments, using only or small relative amounts of MTMOS, showed similar silica leaching levels to conventional materials.[27] However, materials produced with very low levels of CPTMOS, such as the BP-1 made from a ratio of 62:30:1 TMOS:MTMOS:CPTMOS, show strong increases in the level of silica leaching at pH = 10, up to 70.0

ppm for the BP-1. However, the sol–gel materials with very low amounts of CPTMOS also show a decrease in leaching upon polymer grafting (Figure 10). This is thought to be a direct result of the decreased number of Q_3 and T_2 sites upon surface reorganization during the polyamine addition step.

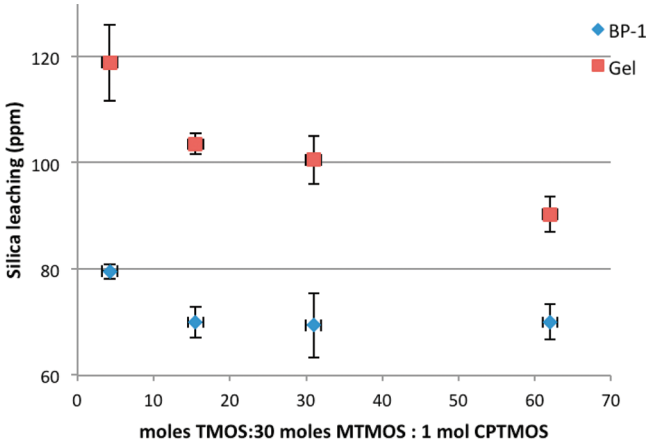

Figure 10. Silica leaching for sol–gels with varying relative amounts of TMOS. All gels showed significantly decreased leaching upon conversion to BP-1.

BP-1 Longevity Studies. The SPC materials made commercially have very long usable lifetimes. An SPC made from commercial silica gel showed <10% loss in capacity after more than 3000 copper loading–acid stripping–base regeneration cycles.[37] This structural durability is maintained with the 62:30:1 sol–gel BP-2, which shows no observed capacity loss in 1000 copper loading–acid stripping–base regeneration cycles with an average breakthrough copper capacity of 27 mg/g at pH = 2 (Supplemental Table 2, Supporting Information).

CONCLUSIONS

A number of important conclusions can be made from the work reported here. Sol–gel materials offer an alternative to amorphous silica gels as a matrix for polyamine composites. Pore size distributions are narrower, and the ability to change the pore size provides additional potential for modification with bulkier ligands. The systematic studies of the reaction conditions for formation of the sol–gel provided insight into mechanisms of pore formation, allowing more effective tailoring of pore size. Both the acid catalyzed step and the base catalyzed step can have significant impacts on pore formation. Silicate leaching at pH = 10 from sol–gel materials is similar to that of conventional silica for the polymer modified composites, but higher concentrations of methyl groups relative to chloropropyl groups increases leaching, as a result of decreased steric hindrance and/or hydrophobicity of the small methyl group. The introduction of TMOS showed improvements in sol–gel composite performance, particularly in providing narrower pore size distributions that also decreases internalization of chloropropyl group and results in increased copper capacities due to better polymer loading. BP-1 and BP-2 copper batch capacities, equal to or greater than those of commercial materials, have been achieved for sol–gel based materials, indicating potential as a replacement material for amorphous silica in some applications. Lower batch copper loading capacities were expressed for sol–gel derived CuSelect, due to low levels of ligand loading thought to be related to a decrease in the number of larger pores needed to accommodate the larger aromatic ligand. Similar or slightly less selectivity was found for ligand modified materials in breakthrough experiments. CuSelect selectivity was 40:1, which is significantly less than the 67:1 for amorphous silica materials. BP-2 selectivity was 11:1 (Cu^{2+}:Ni^{2+}) similar to that observed for the amorphous silica analog . Finally, The durability of the sol–gel SPC compares favorably with the commercially produced materials.

ASSOCIATED CONTENT

Supporting Information

Supplemental Table 1, parameters used for solid-state NMR experiments; supplemental Table 2, sol–gel BP-2 resin longevity test cycle details; supplemental Figure 1, method for calculating the number of surface anchor points per polymer molecule; supplemental Figure 2, ^{29}Si NMR of sol–gel BP-1s with increasing relative amounts of TMOS. This material is available free of charge via the Internet at http://pubs.acs.org.

AUTHOR INFORMATION

Corresponding Author

*E-mail: edward.rosenberg@mso.umt.edu.

Notes

The authors declare no competing financial interest.

ACKNOWLEDGMENTS

We gratefully acknowledge the support of the National Science Foundation (CHE070938 and CHE1049569) and Purity Systems Inc. for their cooperation in this project. Electron microscopy services and resources were provided by the Electron Microscopy Facility, Division of Biological Sciences, University of Montana, Missoula, MT. The EM Facility is supported, in part, by grant #RR-16455-04 from the National Center for Research Resources (Biomedical Research Infrastructure Network program), National Institutes of Health.

REFERENCES

(1) Huang, Y. G.; Jiang, F.-L.; Hong, M.-C. *Coord. Chem. Rev.* **2009**, *253*, 2814.
(2) Yuan, P.; Zhao, L.; Liu, N.; Wei, G.; Zhang, Y.; Wang, Y.; Yu, C. *Chem.–Eur. J.* **2009**, *15*, 11319.
(3) Carniato, F.; Secco, A.; Gatti, G.; Marchese, L.; Sappa, E. *J. Sol-Gel Sci. Technol.* **2009**, *52*, 235.
(4) Banet, P.; Griesmar, P.; Serfaty, S.; Vidal, F.; Jaouen, V.; Le Huerou, J.-Y. *J. Phys. Chem. B* **2009**, *113*, 14914.
(5) Srivastava, V.; Gaubert, K.; Pucheault, M.; Vaultier, M. *Chem. Catal. Chem.* **2009**, *1*, 94.
(6) Kang, D. J.; Bae, B. S. *Acc. Chem. Res.* **2007**, *40*, 903.
(7) Dunn, B.; Zink, J. I. *Acc. Chem. Res.* **2007**, *40* (9), 729.
(8) Ashkenasy, G.; Cahen, D.; Cohen, R.; Shanzer, A.; Vilan, A. *Acc. Chem. Res.* **2002**, *35*, 121.
(9) Tezuka, T.; Tadanaga, K.; Hayashi, A.; Tatsumisago, M. *J. Am. Chem. Soc.* **2006**, *128*, 16470.
(10) Mark, J. E.; Lee, C. Y-C.; Bianconi, P. A. *Hybrid Inorganic-Organic Composites, ACS Symposium Series 585*; ACS: Washington, DC, 1995.
(11) Nalwa, H. S. *Handbook of Organic-Inorganic Hybrid Materials and Nanocomposites*, 2-Vol. Set; Amer. Sci. Pub.: Stevenson Ranch, CA, 2003.
(12) Hughes, M.; Miranda, P.; Nielsen, D.; Rosenberg, E.; Gobetto, R.; Viale, A.; Burton, S. In *Recent Advances and Novel Approaches in Macromolecule-Metal Complexes*; Barbucci, R., Ciardelli, F., Ruggeri, G.; Eds.; Wiley-VCH (Macromolecular Symposia 235): Weinheim, 2006; p 161.

(13) Hughes, M.; Nielsen, D.; Rosenberg, E.; Gobetto, R.; Viale, A.; Burton, S. D. *Ind. Eng. Chem. Res.* **2006**, *45*, 6538−6547.
(14) (a) Hughes, M.; Rosenberg, E. *Sep. Sci. Technol.* **2007**, *42*, 261. (b) Berlin, M.; Allen, J.; Rosenberg, D.; Rosenberg, E.. *Appl. Organomet. Chem.* **2011**, *25*, 530.
(15) Wong, Y. O.; Miranda, P.; Rosenberg, E. *J. Appl. Polym. Sci.* **2010**, *115*, 2855.
(16) Hughes, M. A.; Wood, J.; Rosenberg, E. *Ind. Eng. Chem. Res.* **2008**, *47*, 6765.
(17) Kailasam, V.; Rosenberg, E.; Nielsen, D. *Ind. Eng. Chem. Res.* **2009**, *48*, 3991.
(18) Nielsen, D.; Mckenzie, J.; Clancy, J.; Rosenberg, E. *Chim. Oggi* **2009**, *26*, 42.
(19) Rosenberg, E. In *Macromolecules Containing Metal and Metal Like Elements*; Carraher, C. E., Pittman, C. U., Abd-El-Aziz, A. S., Zeldin, M., Sheats, J. E., Eds.; J. Wiley & Sons: New York, 2005; Vol. *4*, p 51.
(20) Anderson, C.; Rosenberg, E.; Hart, C. K.; Ratz, C. Y. In *Proceedings of the 5th International Symposium on Hydrometallurgy*; Young, C., Ed.; TMS: Warendale, PA, 2003; Vol. *1*, p 393.
(21) Rosenberg, E.; Fischer, R. C.; Hart, C. K. In *2003 EPD Proceedings-Mercury Management*; Schlesinger, M. E., Ed.; TMS: Warendale, PA, 2003; p 285.
(22) Rosenberg, E.; Pang, D. U. S. Patent 5,695,882, 1997.
(23) Rosenberg, E.; Pang, D. U. S. Patent No. 5,997,748, 1999.
(24) Rosenberg, E.; Fischer, R. C. U. S. Patent. No. 6,576,590, 2003.
(25) Rosenberg, E.; Fischer, R. C. U. S. Patent. No.7,008,601, 2006.
(26) Rosenberg, E.; Hart, C. *Proceedings International Water Conference*, Nov. 13−17, 2011, Orlando, FL, IWC-10.
(27) Allen, J.; Berlin, M.; Hughes, M.; Johnston, E.; Kailasam, V.; Rosenberg, E.; Sardot, T.; Wood. *Mater. Chem. Phys* **2011**, *126*, 973.
(28) Prabakar, S.; Assink, R. A. *J. Non-Cryst. Solids* **1997**, *211*, 39.
(29) (a) Van Blaaderen, A.; Vrij, A. *J. Colloid Interface Sci.* **1993**, *156*, 1. (b) Loy, D. A.; Baugher, B. M.; Baugher, C. R. *Chem. Mater.* **2000**, *12*, 3624.
(30) Kresge, C. T.; Leonowicz, M. E.; Roth, W. J.; Vartuli, J. C.; Beck, J. S. *Nature* **1992**, *359*, 710.
(31) Velev, D. O.; Lenhoff, A. M. *Curr. Opin. Colloid Interface Sci.* **2000**, *5*, 56.
(32) Imhof, A.; Pine, D. *J. Adv. Mater.* **1998**, *10*, 697.
(33) Dong, H.; Brennan, J. D. *Chem. Mater.* **2006**, *18*, 541.
(34) Sanchez, J.; Rankin, S. E.; McCormick, A. V. *Ind. Eng. Chem. Res.* **1996**, *35*, 117.
(35) Olejniczak, Z.; Łeczkab, M.; Cholewa-Kowalskab, K.; Wojtachb, K.; Rokitab, M.; Mozgawa, W. *J. Mol. Struct.* **2005**, *744−747*, 465.
(36) Shimojima, A.; Kuroda, K. *Langmuir* **2002**, *18*, 1144.
(37) Beatty, S.; Fischer, R.; Hagers, D.; Rosenberg, E. *Ind. Eng. Chem. Res.* **1999**, *38*, 4402.
(38) Mercier, L.; Pinnavaia, T. *Chem. Mater.* **2000**, *12*, 188.
(39) Rodriguez, S.; Colon, L. *Chem. Mater.* **1999**, *11*, 754.
(40) Gritti, F.; Terrien, I.; Menu, S.; Dufourc, E. J.; Felix, G.; Achard, M.-F.; Hardouin, F. *J. Chromatogr., A* **2001**, *922*, 37.
(41) Rosenberg, E.; Fan, Z.; Li, D. *Yingyong Huaxue* **2003**, *20*, 867.